

# **Lecture Book**

## **B.Sc Mobile Robotics**

D. T. McGuiness, PhD

Version: 2025.SS

(2025, D. T. McGuines, Ph.D)

Current version is 2025.SS.

This document includes the contents of Drive Systems, official name being *Mobile Robotics*, taught at MCI in the Mechatronik Design Innovation. This document is the part of the module MECH-B-4-MRV-MRO-ILV taught in the B.Sc degree.

All relevant code of the document is done using *SageMath* where stated using v10.3 and Python v3.13.1.

This document was compiled with *LuaT<sub>E</sub>X* v1.18.0, and all editing were done using GNU Emacs v29.4 using AUCT<sub>E</sub>X and org-mode package.

This document is based on the books and resources:

The current maintainer of this work along with the primary lecturer  
is D. T. McGuines, Ph.D. (dtm@mci4me.at).

# Contents

<b>I Mechanics of Mobile Robotics</b>	<b>3</b>
<b>1 Perception</b>	<b>5</b>
1.1 Introduction . . . . .	5
1.1.1 Sensors for Mobile Robotics . . . . .	5
1.1.2 Sensor Classification . . . . .	6
1.1.3 Characterising Sensor Performance . . . . .	6
1.1.4 Wheel and Motor Sensors . . . . .	11
1.2 Active Ranging . . . . .	18
1.2.1 The Ultrasonic Sensor . . . . .	19
1.2.2 Motion and Speed Sensors . . . . .	26
1.3 Vision Based Sensors . . . . .	28
1.3.1 CMOS Technology . . . . .	32
1.3.2 Visual Ranging Sensors . . . . .	34
1.3.3 Depth from Focus . . . . .	34
<b>Bibliography</b>	<b>43</b>



# List of Figures

1.1	An example of a rotary encoder. [1]	12
1.2	An example of an electronic compass [2].	13
1.3	Optical Gyroscopes have no moving parts, (unlike mechanical gyroscopes) making them extremely reliable [3].	14
1.4	.....	15
1.5	Signals of an ultrasonic sensor.	19
1.6	An example of an ultrasonic sensor used in Raspberry Pi applications [4].	20
1.7	A laser range finder used in robotics applications	21
1.8	Schematic of laser rangefinding by phase-shift measurement.	22
1.9	Range estimation by measuring the phase shift between transmitted and received signals.	23
1.10	Principle of 1D laser triangulation.	24
1.11	Structured light sources on display at the 2014 Machine Vision Show in Boston [5].	25
1.12	Sony ICX493AQA 10.14-megapixel APS-C (23.4 × 15.6 mm) Charge Coupled Device (CCD) from digital camera Sony DSLR-A200 or DSLR-A300, sensor side [6].	28
1.13	Normalized Spectral Response of a Typical Monochrome CCD.	29
1.14	Types of colour filter used in commercial and industrial applications	30
1.15	Example of white balance. Here the same scene is emulated to be shot under different light conditions [9].	31
1.16	A close-up view of a Complimentary MOS (CMOS) sensor and its circuitry [13].	32
1.17	Photon noise simulation. Number of photons per pixel increases from left to right and from upper row to bottom row [16].	33
1.18	Depiction of the camera optics and its impact on the image. To get a sharp image, the image plane must coincide with the focal plane. Otherwise the image of the point ( $x, y, z$ ) will be blurred in the image as can be seen in the drawing above.	35
1.19	Three images of the same scene taken with a camera at three different focusing positions. Note the significant change in texture sharpness between the near surface and far surface [17].	35



# **List of Tables**



# **Part I**

# **Mechanics of Mobile Robotics**



# Chapter 1

## Perception

### Table of Contents

1.1	Introduction . . . . .	5
1.2	Active Ranging . . . . .	18
1.3	Vision Based Sensors . . . . .	28

### 1.1 Introduction

One of the most important tasks of an Autonomous Mobile Robotics (AMR) is to acquire knowledge about its environment.<sup>1</sup> This is achieved by taking measurements using various sensors and then extracting meaningful information from those measurements.

In this chapter we present the most common sensors used in AMR and then discuss strategies for extracting information from the sensors.

<sup>1</sup>One could even argue it is the definition of life, if you ask a biologist as the ability to feel and act on its environment is the bare necessity.

#### 1.1.1 Sensors for Mobile Robotics

There is a wide variety of sensors used in AMRs (Fig. 4.1). Some are used to measure simple values like the internal temperature of a robot's electronics or the rotational speed of the motors in its wheels or actuators. Other, more sophisticated sensors can be used to acquire information about the robot's environment or even to directly measure a robot's global position. Here, we focus primarily on sensors used to extract information about the robot's environment. Because a AMR moves around, it will frequently encounter unforeseen environmental characteristics, and therefore such sensing is particularly critical. We begin with a functional classification of sensors. Then, after presenting basic tools for describing a sensor's performance, we proceed to describe selected sensors in detail.

### 1.1.2 Sensor Classification

We classify sensors using two (2) important functional axes. Let's define these terms for clarity;

**Proprioceptive** sensors which measure values **internal** to the robot.

e.g., motor speed, wheel load, robot arm joint angles, battery voltage.

**Exteroceptive** sensors which measure information from the **robot's environment**;

e.g., distance measurements, light intensity, sound amplitude.

exteroceptive sensor measurements are interpreted by the robot to extract meaningful environmental features.

**Passive** sensors measure ambient environmental energy entering the sensor.

e.g., temperature probes, microphones and CCD or CMOS cameras.

**Active** sensors emit energy into the environment, then measure the environmental reaction. Because active sensors can manage more controlled interactions with the environment, they often achieve superior performance. However, active sensing introduces several risks: the outbound energy may affect the very characteristics that the sensor is attempting to measure. Furthermore, an active sensor may suffer from interference between its signal and those beyond its control. For example, signals emitted by other nearby robots, or similar sensors on the same robot may influence the resulting measurements. Examples of active sensors include wheel quadrature encoders, ultrasonic sensors and laser rangefinders.

The sensor classes in Table (4.1) are arranged in ascending order of complexity and descending order of technological maturity. Tactile sensors and proprioceptive sensors are critical to virtually all mobile robots, and are well understood and easily implemented. Commercial quadrature encoders, for example, may be purchased as part of a gear-motor assembly used in a AMR. At the other extreme, visual interpretation by means of one or more CCD/CMOS cameras provides a broad array of potential functionalities, from obstacle avoidance and localisation to human face recognition. However, commercially available sensor units that provide visual functionalities are only now beginning to emerge

### 1.1.3 Characterising Sensor Performance

The sensors we describe in this chapter vary greatly in their performance characteristics. Some sensors provide extreme accuracy in well-controlled laboratory settings, but are overcome with error when subjected to real-world environmental variations. Other sensors provide narrow, high precision data in a wide variety settings. To quantify such performance characteristics, first we formally define the sensor performance terminology that will be valuable throughout the rest of this chapter.

## Basic Sensor Response Ratings

A number of sensor characteristics can be rated **quantitatively** in a laboratory setting. Such performance ratings will necessarily be best-case scenarios when the sensor is placed on a real-world robot, but are nevertheless useful.

**Dynamic Range** Used to measure the spread between the lower and upper limits of inputs values to the sensor while maintaining normal sensor operation. Formally, the dynamic range is the ratio of the maximum input value to the minimum measurable input value. Because this raw ratio can be unwieldy, it is usually measured in Decibels, which is computed as ten times the common logarithm of the dynamic range. However, there is potential confusion in the calculation of Decibels, which are meant to measure the ratio between powers, such as Watts or Horsepower.

Suppose your sensor measures motor current and can register values from a minimum of 1 mA to 20 A. The dynamic range of this current sensor is defined as:

$$10 \cdot \log \left[ \frac{20}{0.001} \right] = 43 \text{ dB} \quad (1.1)$$

Now suppose you have a voltage sensor that measures the voltage of your robot's battery, measuring any value from 1 mV to 20 V. Voltage is **NOT** a unit of power, but the square of voltage is proportional to power. Therefore, we use 20 instead of 10:

$$20 \cdot \log \left[ \frac{20}{0.001} \right] = 86 \text{ dB} \quad (1.2)$$

**Range** An important rating in AMR because often robot sensors operate in environments where they are frequently exposed to input values beyond their working range. In such cases, it is critical to understand how the sensor will respond. For example, an optical rangefinder will have a minimum operating range and can thus provide spurious data when measurements are taken with object closer than that minimum.

**Resolution** The minimum difference between two (2) values that can be detected by a sensor. Usually, the lower limit of the dynamic range of a sensor is equal to its resolution. However, in the case of digital sensors, this is not necessarily so. For example, suppose that you have a sensor that measures voltage, performs an analogue-to-digital conversion and outputs the converted value as an 8-bit number linearly corresponding to between 0 and 5 Volts. If this sensor is truly linear, then it has  $2^8 - 1$  total output values or a resolution of:

$$\frac{5}{255} = 20 \text{ mV}$$

**Linearity** is an important measure governing the behaviour of the sensor's output signal as the input signal varies. A linear response indicates that if two (2) inputs, say  $x$  and  $y$  result in the two outputs  $f(x)$  and  $f(y)$ , then for any values  $a$  and  $b$ , the following relation can be derived:

$$f(x + y) = f(x) + f(y).$$

This means that a plot of the sensor's input/output response is simply a straight line.

**Bandwidth or Frequency** is used to measure the speed with which a sensor can provide a stream of readings. Formally, the number of measurements per second is defined as the sensor's frequency in Hz. Because of the dynamics of moving through their environment, mobile robots often are limited in maximum speed by the bandwidth of their obstacle detection sensors. Thus increasing the bandwidth of ranging and vision-based sensors has been a high-priority goal in the robotics community.

### In Situ Sensor Performance

The above sensor characteristics can be reasonably measured in a laboratory environment, with confident extrapolation to performance in real-world deployment. However, a number of important measures cannot be reliably acquired without deep understanding of the complex interaction between all environmental characteristics and the sensors in question. This is most relevant to the most sophisticated sensors, including active ranging sensors and visual interpretation sensors.

**Sensitivity** A measure of the degree to which an incremental change in the target input signal changes the output signal. Formally, sensitivity is the ratio of output change to input change. Unfortunately, however, the sensitivity of exteroceptive sensors is often confounded by undesirable sensitivity and performance coupling to other environmental parameters.

**Cross-Sensitivity** is the technical term for sensitivity to environmental parameters that are orthogonal to the target parameters for the sensor. For example, a flux-gate compass can demonstrate high sensitivity to magnetic north and is therefore of use for AMR navigation. However, the compass will also demonstrate high sensitivity to ferrous building materials, so much so that its cross-sensitivity often makes the sensor useless in some indoor environments. High cross-sensitivity of a sensor is generally undesirable, especially so when it cannot be modelled.

**Error** of a sensor is defined as the difference between the sensor's output measurements and the true values being measured, within some specific operating context.

As an example, given a true value  $v$  and a measured value  $m$ , we can define error as:

$$\text{Error} = m - v.$$

**Accuracy** defined as the degree of conformity between the sensor's measurement and the true value, and is often expressed as a proportion of the true value (e.g. 97.5% accuracy):

$$\text{Accuracy} = 1 - \frac{|m - v|}{v}.$$

Of course, obtaining the ground truth ( $v$ ), can be difficult or impossible, and so establishing a confident characterisation of sensor accuracy can be problematic. Further, it is important to distinguish between two different sources of error:

- Systematic errors are caused by factors or processes that can in theory be modelled. These errors are, therefore, deterministic.<sup>2</sup>

Poor calibration of a laser rangefinder, un-modelled slope of a hallway floor and a bent stereo camera head due to an earlier collision are all possible causes of systematic sensor errors

<sup>2</sup>Meaning, it's value is not determined by a random process and therefore should, in theory, be predictable.

- Random errors cannot be predicted using a sophisticated model nor can they be mitigated with more precise sensor machinery. These errors can only be described in probabilistic terms (i.e. stochastic). Hue instability in a colour camera, spurious range-finding errors and black level noise in a camera are all examples of random errors.

**Precision** is often confused with accuracy, and now we have the tools to clearly distinguish these two terms. Intuitively, high precision relates to reproducibility of the sensor results. For example, one sensor taking multiple readings of the same environmental state has high precision if it produces the same output. In another example, multiple copies of this sensors taking readings of the same environmental state have high precision if their outputs agree. Precision does not, however, have any bearing on the accuracy of the sensor's output with respect to the true value being measured. Suppose that the random error of a sensor is characterised by some mean value ( $\mu$ ) and a standard deviation ( $\sigma$ ). The formal definition of precision is the ratio of the sensor's output range to the standard deviation:

$$\text{Precision} = \frac{\text{Range}}{\sigma}.$$

Only  $\sigma$  and **NOT**  $\mu$  has impact on precision. In contrast mean error is directly proportional to overall sensor error and inversely proportional to sensor accuracy.

## Characterising Error

Mobile robots depend heavily on **exteroceptive** sensors. Many of these sensors concentrate on a central task for the robot:

*acquiring information on objects in the robot's immediate vicinity so that it may interpret the state of its surroundings.*

Of course, these "objects" surrounding the robot are all detected from the viewpoint of its local reference frame.<sup>3</sup> Since the systems we study are **mobile**, their ever-changing position and their motion has a significant impact on overall sensor behaviour.

<sup>3</sup>In this case we are referring to the robot reference frame.

Now that we have the necessary knowledge on the fundamental concepts and terminology, we can now describe how dramatically the sensor error of an AMR **disagrees** with the ideal picture drawn in the previous section.

## Blurring of Systematical and Random Errors

Active ranging sensors tend to have failure modes which are triggered largely by specific relative positions of the sensor and environment targets.

<sup>4</sup>The incident light is reflected into a single outgoing direction.

For example, a sonar sensor will produce specular reflections,<sup>4</sup> producing grossly inaccurate measurements of range, at specific angles to a smooth sheet-rock wall.

During motion of the robot, such relative angles occur at stochastic intervals. This is especially true in a AMR outfitted with a ring of multiple sonars. The chances of one sonar entering this error mode during robot motion is high. From the perspective of the moving robot, the sonar measurement error is a **random error** in this case. However, if the robot were to stop, becoming motionless, then a very different error modality is possible.

If the robot's static position causes a particular sonar to fail in this manner, the sonar will fail consistently and will tend to return precisely the same (and incorrect!) reading time after time. Once the robot is motionless, the error appears to be systematic and high precision.

The fundamental mechanism at work here is the cross-sensitivity of AMR sensors to robot pose and robot-environment dynamics.

The models for such cross-sensitivity are **NOT**, in an underlying sense, truly random. However, these physical interrelationships are rarely modelled and therefore, from the point of view of an incomplete model, the errors appear random during motion and systematic when the robot is at rest. Sonar is not the only sensor subject to this blurring of systematic and random error modality. Visual interpretation through the use of a CCD camera is also highly susceptible to robot motion and position because of camera dependency on lighting.<sup>5</sup>

<sup>5</sup>such as glare and reflections.

The important point is to realise that, while systematic error and random error are well-defined in a controlled setting, the AMR can exhibit error characteristics that bridge the gap between deterministic and stochastic error mechanisms.

## Multi-Modal Error Distributions

It is common to characterise the behaviour of a sensor's random error in terms of a probability distribution over various output values. In general, one knows very little about the causes of random error and therefore several simplifying assumptions are commonly used. For example, we can assume that the error is zero-mean ( $\mu = 0$ ), in that it symmetrically generates both positive and negative measurement error. We can go even further and assume that the probability density curve is Gaussian. Although we discuss the mathematics of this in detail later, it is important for now to recognise the fact that one frequently assumes symmetry as well as unimodal distribution. This means that measuring the correct value is most probable, and any measurement that is further away from the correct value is less likely than any measurement that is closer to the correct value. These are strong

assumptions that enable powerful mathematical principles to be applied to AMR problems, but it is important to realise how wrong these assumptions usually are.

Consider, for example, the sonar sensor once again. When ranging an object that reflects the sound signal well, the sonar will exhibit high accuracy, and will induce random error based on noise, for example, in the timing circuitry. This portion of its sensor behaviour will exhibit error characteristics that are fairly **symmetric** and **unimodal**. However, when the sonar sensor is moving through an environment and is sometimes faced with materials that cause coherent reflection rather than returning the sound signal to the sonar sensor, then the sonar will grossly overestimate distance to the object. In such cases, the error will be biased toward positive measurement error and will be far from the correct value. The error is not strictly systematic, and so we are left modelling it as a probability distribution of random error. So the sonar sensor has two (2) separate types of operational modes, one in which the signal does return and some random error is possible, and the second in which the signal returns after a multi-path reflection, and gross overestimation error occurs. The probability distribution could easily be at least bimodal in this case, and since overestimation is more common than underestimation it will also be asymmetric.

As a second example, consider ranging via stereo vision. Once again, we can identify two (2) modes of operation. If the stereo vision system correctly correlates two images, then the resulting random error will be caused by camera noise and will limit the measurement accuracy. But the stereo vision system can also correlate two images incorrectly, matching two fence posts for example that are not the same post in the real world. In such a case stereo vision will exhibit gross measurement error, and one can easily imagine such behaviour violating both the unimodal and the symmetric assumptions. The thesis of this section is that sensors in a AMR may be subject to multiple modes of operation and, when the sensor error is characterised, uni modality and symmetry may be grossly violated. Nonetheless, as you will see, many successful AMR systems make use of these simplifying assumptions and the resulting mathematical techniques with great empirical success. The above sections have presented a terminology with which we can characterise the advantages and disadvantages of various mobile robot sensors. In the following sections, we do the same for a sampling of the most commonly used AMR sensors today.

### 1.1.4 Wheel and Motor Sensors

Wheel/motor sensors are devices used to measure the internal state and dynamics of a mobile robot. These sensors have vast applications outside of AMR and, as a result, AMR has enjoyed the benefits of high-quality, low-cost wheel and motor sensors which offer excellent resolution.

In the next part, we sample just one such sensor, the optical incremental encoder.

## Optical Encoders

Optical incremental encoders have become the most popular device for measuring angular speed and position within a motor drive or at the shaft of a wheel or steering mechanism. In mobile robotics, encoders are used to control the position or speed of wheels and other motor-driven joints. Because these sensors are proprioceptive, their estimate of position is best in the reference frame of the robot and, when applied to the problem of robot localisation, significant corrections are required as discussed in Chapter 5.

An optical encoder is basically a mechanical light chopper that produces a certain number of sine or square wave pulses for each shaft revolution. It consists of an illumination source, a fixed grating that masks the light, a rotor disc with a fine optical grid that rotates with the shaft, and fixed optical detectors. As the rotor moves, the amount of light striking the optical detectors varies based on the alignment of the fixed and moving gratings. In robotics, the resulting sine wave is transformed into a discrete square wave using a threshold to choose between light and dark states. Resolution is measured in Cycles Per Revolution (CPR).

The minimum angular resolution can be readily computed from an encoder's CPR rating. A typical encoder in AMR may have 2,000 CPR while the optical encoder industry can readily manufacture encoders with 10,000 CPR. In terms of required bandwidth, it is of course critical that the encoder be sufficiently fast to count at the shaft spin speeds that are expected. Industrial optical encoders present no bandwidth limitation to AMR applications. Usually in AMR the quadrature encoder is used. In this case, a second illumination and detector pair is placed 90° shifted with respect to the original in terms of the rotor disc. The resulting twin square waves, shown in Fig. 4.2, provide significantly more information. The ordering of which square wave produces a rising edge first identifies the direction of rotation. Furthermore, the four detectability different states improve the resolution by a factor of four with no change to the rotor disc. Thus, a 2,000 CPR encoder in quadrature yields 8,000 counts. Further improvement is possible by retaining the sinusoidal wave measured by the optical detectors and performing sophisticated interpolation. Such methods, although rare in AMR, can yield 1000-fold improvements in resolution. As with most proprioceptive sensors, encoders are generally in the controlled environment of a AMR's internal structure, and so systematic error and cross-sensitivity can be engineered away. The accuracy of optical encoders is often assumed to be 100% and, although this may not entirely correct, any errors at the level of an optical encoder are dwarfed by errors downstream of the motor shaft.



Figure 1.1: An example of a rotary encoder. [1]

## Heading Sensors

Heading sensors can be proprioceptive (gyroscope, inclinometer) or exteroceptive (compass). They are used to determine the robots orientation and inclination. They allow us, together with appropriate velocity information, to integrate the movement to a position estimate. This procedure,

which has its roots in vessel and ship navigation, is called dead reckoning.

## Compasses

The two most common modern sensors for measuring the direction of a magnetic field are the Hall Effect and Flux Gate compasses. Each has advantages and disadvantages, as described below. The Hall Effect describes the behaviour of electric potential in a semiconductor when in the presence of a magnetic field. When a constant current is applied across the length of a semi-conductor, there will be a voltage difference in the perpendicular direction, across the semi-conductor's width, based on the relative orientation of the semiconductor to magnetic flux

lines. In addition, the sign of the voltage potential identifies the direction of the magnetic field. Thus, a single semiconductor provides a measurement of flux and direction along one dimension. Hall Effect digital compasses are popular in AMR, and contain two such semiconductors at right angles, providing two axes of magnetic field (thresholded) direction, thereby yielding one of 8 possible compass directions. The instruments are inexpensive but also suffer from a range of disadvantages. Resolution of a digital hall effect compass is poor. Internal sources of error include the nonlinearity of the basic sensor and systematic bias errors at the semiconductor level. The resulting circuitry must perform significant filtering, and this lowers the bandwidth of hall effect compasses to values that are slow in AMR terms. For example the hall effect compasses pictured in figure 4.3 needs 2.5 seconds to settle after a 90° spin. The Flux Gate compass operates on a different principle. Two small coils are wound on fer- rite cores and are fixed perpendicular to one-another. When alternating current is activated in both coils, the magnetic field causes shifts in the phase depending upon its relative alignment with each coil. By measuring both phase shifts, the direction of the magnetic field in two dimensions can be computed. The flux-gate compass can accurately measure the strength of a magnetic field and has improved resolution and accuracy; however it is both larger and more expensive than a Hall Effect compass. Regardless of the type of compass used, a major drawback concerning the use of the Earth's magnetic field for AMR applications involves disturbance of that magnetic field by other magnetic objects and man-made structures, as well as the bandwidth limitations of electronic compasses and their susceptibility to vibration. Particularly in indoor environments AMR applications have often avoided the use of compasses, although a compass can conceivably provide useful local orientation information indoors, even in the presence of steel structures.

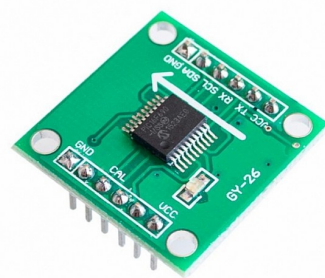


**Figure 1.2:** An example of an electronic compass [2].

## Gyroscope

Gyroscopes are heading sensors which preserve their orientation in relation to a fixed reference frame. Thus they provide an absolute measure for the heading of a mobile system. Gyroscopes

can be classified in two categories, mechanical gyroscopes and optical gyroscopes.

### Mechanical Gyroscopes

The concept of a mechanical gyroscope relies on the inertial properties of a fast spinning rotor. The property of interest is known as the gyroscopic precession. If you try to rotate a fast spinning wheel around its vertical axis, you will feel a harsh reaction in the horizontal axis. This is due to the angular momentum associated with a spinning wheel and will keep the axis of the gyroscope inertially stable. The reactive torque  $\tau$  and thus the tracking stability with the inertial frame are proportional to the spinning speed  $\omega$ , the precession speed  $\Omega$  and the wheel's inertia  $I$ .

$$\tau = I\omega\Omega$$

By arranging a spinning wheel as seen in Figure 4.4, no torque can be transmitted from the outer pivot to the wheel axis. The spinning axis will therefore be space-stable (i.e. fixed in an inertial reference frame). Nevertheless, the remaining friction in the bearings of the gyro- axis introduce small torques, thus limiting the long term space stability and introducing small errors over time. A high quality mechanical gyroscope can cost up to \$100,000 and has an angular drift of about 0.1̄ in 6 hours. For navigation, the spinning axis has to be initially selected. If the spinning axis is aligned with the north-south meridian, the earth's rotation has no effect on the gyro's horizontal axis. If it points east-west, the horizontal axis reads the earth rotation. Rate gyros have the same basic arrangement as shown in Figure 4.4 but with a slight modification. The gimbals are restrained by a torsional spring with additional viscous damping. This enables the sensor to measure angular speeds instead of absolute orientation.

### Optical Gyroscopes

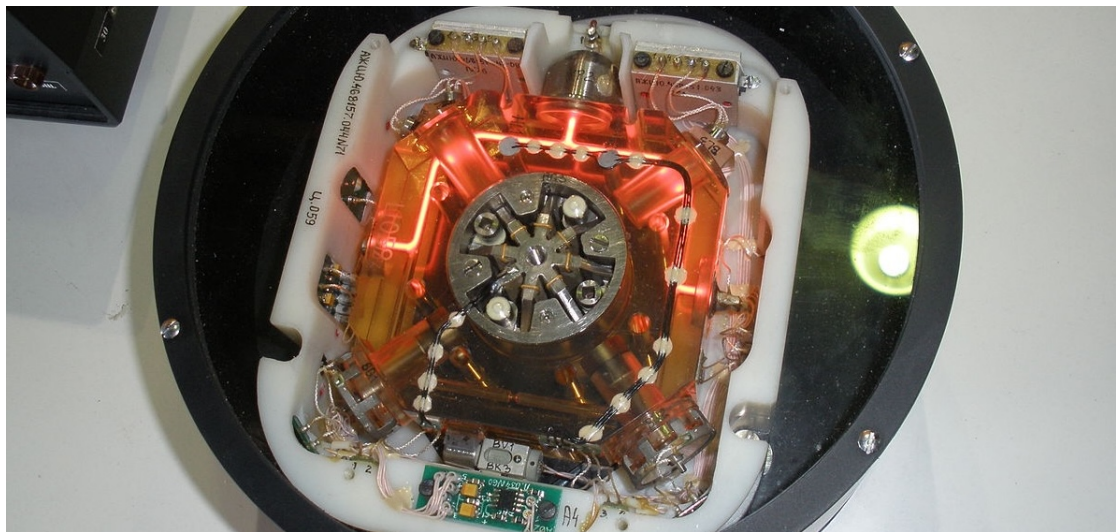


Figure 1.3: Optical Gyroscopes have no moving parts, (unlike mechanical gyroscopes) making them extremely reliable [3].

Optical gyroscopes are a relatively new innovation. Commercial use began in the early 1980's when they were first installed in aircraft. Optical gyroscopes are angular speed sensors that use two monochromatic light beams, or lasers, emitted from the same source instead of moving, mechanical parts. They work on the principle that the speed of light remains unchanged and, therefore, geometric change can cause light to take a varying amount of time to reach its destination. One laser beam is sent traveling clockwise through a fiber while the other travels counterclockwise. Because the laser traveling in the direction of rotation has a slightly shorter path, it will have a higher frequency. The difference in frequency of the two beams is proportional to the angular velocity of the cylinder. New solid-state optical gyroscopes based on the same principle are built using microfabrication technology, thereby providing heading information with resolution and bandwidth far beyond the needs of mobile robotic applications. Bandwidth, for instance, can easily exceed 100KHz while resolution can be smaller than 0.0001°/hr.

### Ground Based Beacons



Figure 1.4

One elegant approach to solving the localization problem in AMR is to use active or passive beacons. Using the interaction of on-board sensors and the environmental beacons, the robot can identify its position precisely. Although the general intuition is identical to that of early human navigation beacons, such as stars, mountains and lighthouses, modern technology has enabled sensors to localize an outdoor robot with accuracies of better than 5 cm within areas that are kilometres in size.

In the following subsection, we describe one such beacon system, the Global Positioning System (GPS), which is extremely effective for outdoor ground-based and flying robots. Indoor beacon systems have been generally less successful for a number of reasons. The expense of environmental modification in an indoor setting is not amortized over an extremely large useful area, as it is for example in the case of GPS. Furthermore, indoor environments offer significant challenges not seen outdoors, including multipath and environment dynamics. A laser-based indoor beacon system, for example, must disambiguate the one true laser signal from possibly tens of other powerful signals that have reflected off of walls, smooth floors and doors. Confounding this, humans and other obstacles

may be constantly changing the environment, for example occluding the one true path from the beacon to the robot. In commercial applications such as manufacturing plants, the environment can be carefully controlled to ensure success. In less structured indoor settings, beacons have nonetheless been used, and the problems are mitigated by careful beacon placement and the useful of passive sensing modalities.

### Global Positioning System

The Global Positioning System (GPS) was initially developed for military use but is now freely available for civilian navigation. There are at least 24 operational GPS satellites at all times. The satellites orbit every 12 hours at a height of 20.190km. There are four (4) satellites which located in each of six planes inclined 55° with respect to the plane of the earth's equator (figure 4.5).

Each satellite continuously transmits data which indicates its location and the current time. Therefore, GPS receivers are **completely passive** but **exteroceptive** sensors. The GPS satellites synchronise their transmissions to allow their signals to be sent at the same time. When a GPS receiver reads the transmission of two (2) or more satellites, the arrival time differences inform the receiver as to its relative distance to each satellite.

By combining information regarding the arrival time and instantaneous location of four (4) satellites, the receiver can infer its own position.

In theory, such triangulation requires only three (3) data points. However, timing is extremely critical in the GPS application because the time intervals being measured are in ns.

It is, of course, mandatory the satellites to be well synchronised. To this end, they are updated by ground stations regularly and each satellite carries on-board atomic clocks<sup>6</sup> for timing. The GPS receiver clock is also important so that the travel time of each satellite's transmission can be accurately measured. But GPS receivers have a simple quartz clock. So, although 3 satellites would ideally provide position in three axes, the GPS receiver requires 4 satellites, using the additional information to solve for 4 variables: three position axes plus a time correction. The fact that the GPS receiver must read the transmission of 4 satellites simultaneously is a significant limitation. GPS satellite transmissions are extremely low-power, and reading them successfully requires direct line-of-sight communication with the satellite. Thus, in confined spaces such as city blocks with tall buildings or dense forests, one is unlikely to receive 4 satellites reliably. Of course, most indoor spaces will also fail to provide sufficient visibility of the sky for a GPS receiver to function. For these reasons, GPS has been a popular sensor in AMR, but has been relegated to projects involving AMR traversal of wide-open spaces and autonomous flying machines. A number of factors affect the performance of a localization sensor that makes use of GPS. First, it is important to understand that, because of the specific orbital paths of the GPS satellites, coverage is not geometrically identical in different portions of the Earth and therefore resolution is not uniform. Specifically, at the North and South poles, the satellites are very close to the horizon and, thus, while resolution in the latitude and longitude directions is good, resolution of altitude is relatively poor as compared to



<sup>6</sup>An example of a cesium clock for use in GPS.

more equatorial locations.

The second point is that GPS satellites are merely an information source. They can be employed with various strategies in order to achieve dramatically different levels of localisation resolution. The basic strategy for GPS use, called pseudorange and described above, generally performs at a resolution of 15m. An extension of this method is differential GPS, which makes use of a second receiver that is static and at a known exact position. A number of errors can be corrected using this reference, and so resolution improves to the order of 1m or less. A disadvantage of this technique is that the stationary receiver must be installed, its location must be measured very carefully and of course the moving robot must be within kilometers of this static unit in order to benefit from the DGPS technique. A further improved strategy is to take into account the phase of the carrier signals of each received satellite transmission. There are two carriers, at 19cm and 24cm, therefore significant improvements in precision are possible when the phase difference between multiple satellites is measured successfully. Such receivers can achieve 1cm resolution for point positions and, with the use of multiple receivers as in DGPS, sub-1cm resolution. A final consideration for AMR applications is bandwidth. GPS will generally offer no better than 200 - 300ms latency, and so one can expect no better than 5Hz GPS updates. On a fast-moving AMR or flying robot, this can mean that local motion integration will be required for proper control due to GPS latency limitations.

## 1.2 Active Ranging

Active range sensors continue to be the most popular sensors used in AMR. Many ranging sensors have a low price point, and most importantly all ranging sensors provide easily interpreted outputs:

Direct measurements of distance from the robot to objects in its vicinity.

For obstacle detection and avoidance, most AMR rely heavily on active ranging sensors. But the local free-space information provided by range sensors can also be accumulated into representations beyond the robot's current local reference frame. Therefore, active range sensors are also commonly found as part of the localisation and environmental modelling processes of AMRs.

It is only with the slow advent of successful visual interpretation competency that we can expect the class of active ranging sensors to gradually lose their primacy as the sensor class of choice among AMR engineers.

Below, we present two (2) Time-of-Flight (ToF) active range sensors:

- the ultrasonic sensor,
- the laser rangefinder.

Continuing onwards, we then present two (2) geometric active range sensors:

- the optical triangulation sensor,
- the structured light sensor.

### Time-of-Flight Active Ranging

ToF ranging makes use of the [propagation speed of sound](#) or an [electromagnetic wave](#). In general, the travel distance of a sound or electromagnetic wave is given by:

$$d = ct,$$

where  $d$  is the distance travelled usually round-trip (m),  $c$  the speed of wave propagation ( $\text{ms}^{-1}$ ), and  $t$  is the time it takes to travel (s).

It is important to point out the propagation speed  $v$  of sound is approximately  $0.3 \text{ m ms}^{-1}$  whereas the speed of an electromagnetic signal is  $0.3 \text{ m ns}^{-1}$ , which is one million times faster. The ToF for a typical distance, say 3 m, is 10 ms for an ultrasonic system but only 10 ns for a laser rangefinder. It is therefore obvious that measuring the time of flight  $t$  with electromagnetic signals is more technologically challenging.<sup>7</sup>

The quality of ToF range sensors depends mainly on the following:

- Uncertainties in determining the exact time of arrival of the reflected signal,

<sup>7</sup>This explains why laser range sensors have only recently become affordable and robust for use on mobile robots.

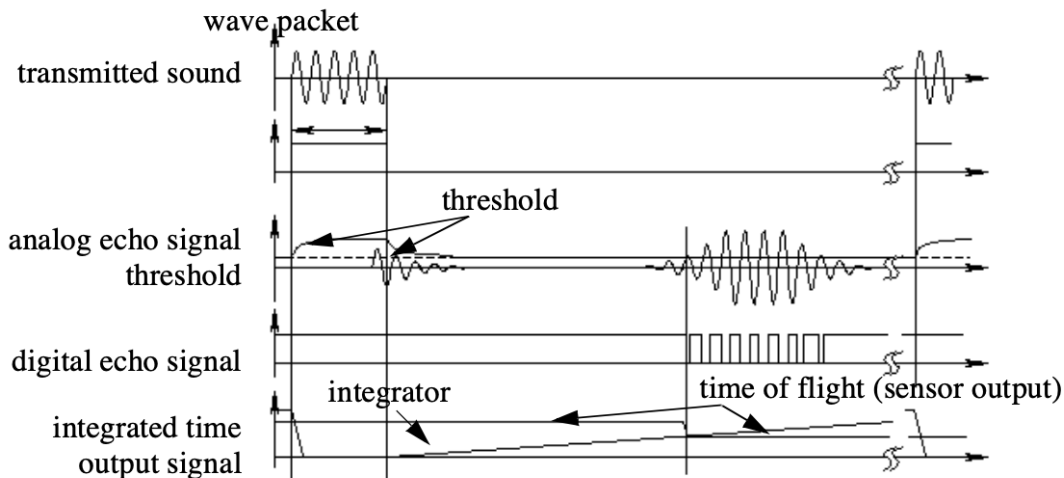


Figure 1.5: Signals of an ultrasonic sensor.

- Inaccuracies in the time of flight measurement, particularly with laser range sensors,
- The dispersal cone of the transmitted beam mainly with ultrasonic range sensors
- Interaction with the target (e.g., surface absorption, specular reflections)
- Variation of propagation speed, and
- The speed of the AMR and target (in the case of a dynamic target).

As discussed below, each type of ToF sensor is sensitive to a particular subset of the above list of factors.

### 1.2.1 The Ultrasonic Sensor

The main ethos of an ultrasonic sensor is to transmit a packet of ultrasonic pressure waves and to measure the time it takes for this wave to reflect and return to the receiver. The distance  $d$  of the object causing the reflection can be calculated based on the propagation speed of sound<sup>8</sup>  $c$  and the time of flight  $t$ .

$$d = \frac{c \times t}{2}$$

The speed of sound ( $v$ ) in air is given by the following relation:

$$v = \sqrt{\gamma RT}$$

where  $\gamma$  is the ratio of specific heat,  $R$  is the gas constant ( $\text{J mol}^{-1} \text{K}^{-1}$ ), and  $T$  is the temperature in Kelvin (K). In air, at standard pressure, and 20 °C the speed of sound is approximately:

$$v = 343 \text{ ms}^{-1}.$$

<sup>8</sup>Of course in this regard careful consideration needs to be made if the medium is significantly different than that of air (i.e., water).

We can see the different signal output and input of an ultrasonic sensor in **Fig. 1.5**.

First, a series of sound pulses are emitted, which creates the wave packet. An integrator also begins to **linearly climb** in value, measuring the time from the transmission of these sound waves to detection of an echo. A threshold value is set for triggering an incoming sound wave as a valid echo.

This threshold is often decreasing in time, because the amplitude of the expected echo decreases over time based on dispersal as it travels longer.

But during transmission of the initial sound pulses and just afterwards, the threshold is set very high to suppress triggering the echo detector with the outgoing sound pulses. A transducer will continue to ring for up to several ms after the initial transmission, and this governs the blanking time of the sensor.

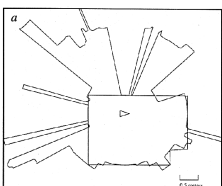
If, during the blanking time, the transmitted sound were to reflect off of an extremely close object and return to the ultrasonic sensor, it may fail to be detected.

However, once the blanking interval has passed, the system will detect any above-threshold reflected sound, triggering a digital signal and producing the distance measurement using the integrator value.

The ultrasonic wave typically has a frequency between 40 and 180 kHz and is usually generated by a piezo or electrostatic transducer. Often the same unit is used to measure the reflected signal, although the required blanking interval can be reduced through the use of separate output and input devices. Frequency can be used to select a useful range when choosing the appropriate ultrasonic sensor for a AMR. Lower frequencies correspond to a longer range, but with the disadvantage of longer post-transmission ringing and, therefore, the need for longer blanking intervals.

Most ultrasonic sensors used by AMRs have an effective range of roughly 12 cm to 5 metres. The published accuracy of commercial ultrasonic sensors varies between 98% and 99.1%. In AMR applications, specific implementations generally achieve a resolution of approximately 2 cm.

In most cases one may want a narrow opening angle for the sound beam in order to also obtain precise directional information about objects that are encountered. This is a major limitation since sound propagates in a cone-like manner with opening angles around  $20^\circ$  and  $40^\circ$ . Consequently, when using ultrasonic ranging one does not acquire depth data points but, rather, entire regions of constant depth. This means that the sensor tells us only that there is an object at a certain distance in within the area of the measurement cone. The sensor readings must be plotted as segments of an arc (sphere for 3D) and not as point measurements.<sup>9</sup> However, recent research developments show significant improvement of the measurement quality in using sophisticated echo processing. Ultrasonic sensors suffer from several additional drawbacks, namely in the areas of **error**, **bandwidth** and **cross-sensitivity**. The published accuracy values for ultrasonic sensors are nominal values based



<sup>9</sup>The results of a 360° scan of a room.



**Figure 1.6:** An example of an ultrasonic sensor used in Raspberry Pi applications [4].

on successful, perpendicular reflections of the sound wave off an acoustically reflective material.

This does not capture the effective error modality seen on a AMR moving through its environment. As the ultrasonic transducer's angle to the object being ranged varies away from perpendicular, the chances become good that the sound waves will coherently reflect away from the sensor, just as light at a shallow angle reflects off of a mirror. Therefore, the true error behavior of ultrasonic sensors is compound, with a well-understood error distribution near the true value in the case of a successful retro-reflection, and a more poorly-understood set of range values that are grossly larger than the true value in the case of coherent reflection.

Of course the acoustic properties of the material being ranged have direct impact on the sensor's performance. Again, the impact is discrete, with one material possibly failing to produce a reflection that is sufficiently strong to be sensed by the unit. For example, foam, fur and cloth can, in various circumstances, acoustically absorb the sound waves. A final limitation for ultrasonic ranging relates to bandwidth. Particularly in moderately open spaces, a single ultrasonic sensor has a relatively slow cycle time.

For example, measuring the distance to an object that is 3 m away will take such a sensor 20ms, limiting its operating speed to 50 Hz. But if the robot has a ring of 20 ultrasonic sensors, each firing sequentially and measuring to minimize interference between the sensors, then the ring's cycle time becomes 0.4s and the overall update frequency of any one sensor is just 2.5 Hz. For a robot conducting moderate speed motion while avoiding obstacles using ultrasonic sensor, this update rate can have a measurable impact on the maximum speed possible while still sensing and avoiding obstacles safely.

## Laser Rangefinder

The laser rangefinder is a ToF sensor which achieves significant improvements over the ultrasonic range sensor due to the [use of laser light instead of sound](#). This type of sensor consists of a transmitter which illuminates a target with a <sup>10</sup> collimated beam (e.g. laser), and a receiver capable of detecting the component of light which is essentially coaxial with the transmitted beam. Often referred to as optical radar or Light Detection and Ranging (LIDAR), these devices produce a range estimate based on the time needed for the light to reach the target and return.

A mechanical mechanism with a mirror sweeps the light beam to cover the required scene in a plane or even in 3 dimensions, using a rotating, nodding mirror. One way to measure the ToF for the light beam is to use a pulsed laser and then measured the elapsed time directly, just as in the ultrasonic solution described in just a little bit. Electronics capable of resolving ps are required in such devices and they are therefore very expensive. A second method is to measure the beat frequency between a frequency modulated continuous wave and its received reflection. Another, even easier

<sup>10</sup>meaning all the rays in questions are made accurately parallel.



Figure 1.7: A laser range finder used in robotics applications

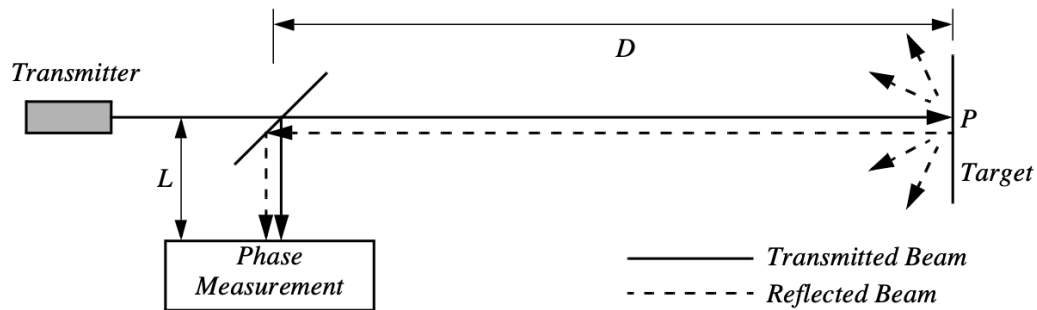


Figure 1.8: Schematic of laser rangefinding by phase-shift measurement.

method is to measure the phase shift of the reflected light.

**Continuous Wave Radar** It is a type of radar system where a known stable frequency continuous wave radio energy is transmitted and then received from any reflecting objects. Individual objects can be detected using the Doppler effect, which causes the received signal to have a different frequency from the transmitted signal, allowing it to be detected by filtering out the transmitted frequency.

Doppler-analysis of radar returns can allow the filtering out of slow or non-moving objects, thus offering immunity to interference from large stationary objects and slow-moving clutter. This makes it particularly useful for looking for objects against a background reflector, for instance, allowing a high-flying aircraft to look for aircraft flying at low altitudes against the background of the surface. Because the very strong reflection off the surface can be filtered out, the much smaller reflection from a target can still be seen.

**Phase Shift Measurement** Near infrared light, which could be from an Light-Emitting Diode (LED) or a laser, is collimated and transmitted from the transmitter  $T$  in Fig. 1.8 and hits a point  $P$  in the environment.

For surfaces having a roughness greater than the wavelength of the incident light, diffuse reflection will occur, meaning that the light is reflected almost isotropically<sup>11</sup>. The wavelength of the infrared light emitted is 824 nm and so most surfaces with the exception of only highly polished reflecting objects, will be diffuse reflectors. The component of the infrared light which falls within the receiving aperture of the sensor will return almost parallel to the transmitted beam, for distant objects. The sensor transmits 100% amplitude modulated light at a known frequency and measures the phase shift between the transmitted and reflected signals.

**Fig. 1.9** shows how this technique can be used to measure range. The wavelength of the modulating signal obeys the equation  $c = f\lambda$  where  $c$  is the speed of light and  $f$  the modulating frequency.

For example,  $f = 5$  MHz, the wavelength is  $\lambda = 60$  m.

<sup>11</sup>Something that is isotropic has the same size or physical properties when it is measured in different directions

The total distance  $D'$  covered by the emitted light is:

$$D' = L + 2D = L \frac{\theta}{2\pi} \lambda$$

where  $D$  and  $L$  are the distances defined in **Fig. 1.8**. The required distance  $D$ , between the beam splitter and the target, is therefore given by:

$$D = \frac{\lambda}{4\pi} \theta$$

where  $\theta$  is the electronically measured phase difference between the transmitted and reflected light beams, and  $\lambda$  the known modulating wavelength. It can be seen that the transmission of a single frequency modulated wave can theoretically result in ambiguous range estimates since

For example if  $\lambda = 60\text{m}$ , a target at a range of  $5\text{ m}$  would give an indistinguishable phase measurement from a target at  $65\text{ m}$ , since each phase angle would be  $360^\circ$  apart.

We therefore define an **ambiguity interval** of  $\lambda$ , but in practice we note that the range of the sensor is much lower than  $\lambda$  due to the attenuation of the signal in air. It can be shown that the confidence in the range (phase estimate) is inversely proportional to the square of the received signal amplitude, directly affecting the sensor's accuracy. Hence dark, distant objects will not produce as good range estimates as close, bright objects.

As with ultrasonic ranging sensors, an important error mode involves coherent reflection of the energy. With light, this will only occur when striking a highly polished surface. Practically, a AMR may encounter such surfaces in the form of a polished desktop, file cabinet or of course a mirror. Unlike ultrasonic sensors, laser rangefinders cannot detect the presence of optically transparent materials such as glass, and this can be a significant obstacle in environments, for example museums, where glass is commonly used.

### Triangulation-based Active Ranging

Triangulation-based ranging sensors use geometrical properties in their measuring strategy to establish distance readings to objects. The simplest class of triangulation-based rangers are active because they project a known light pattern (e.g., a point, a line or a texture) onto the environment. The

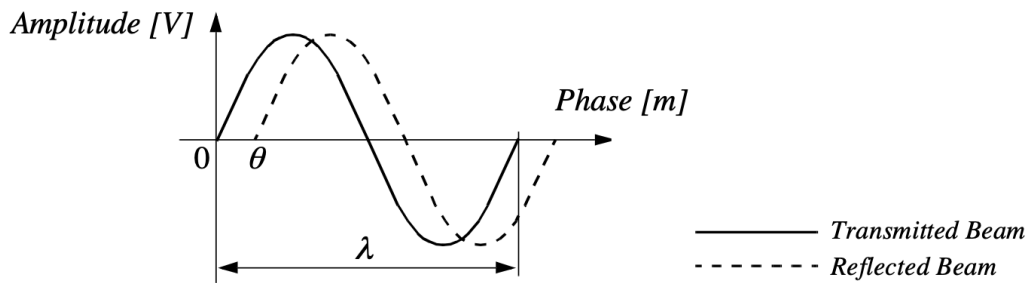


**Figure 1.9:** Range estimation by measuring the phase shift between transmitted and received signals.

reflection of the known pattern is captured by a receiver and, together with known geometric values, the system can use simple triangulation to establish range measurements. If the receiver measures the position of the reflection along a single axis, we call the sensor an optical triangulation sensor in 1D. If the receiver measures the position of the reflection along two orthogonal axes, we call the sensor a structured light sensor. These two (2) sensor types are described in the two subsections below.

### Optical Triangulation (1D Sensor)

The principle of optical triangulation in 1D is straightforward, as depicted in **Fig. 1.10**. A collimated

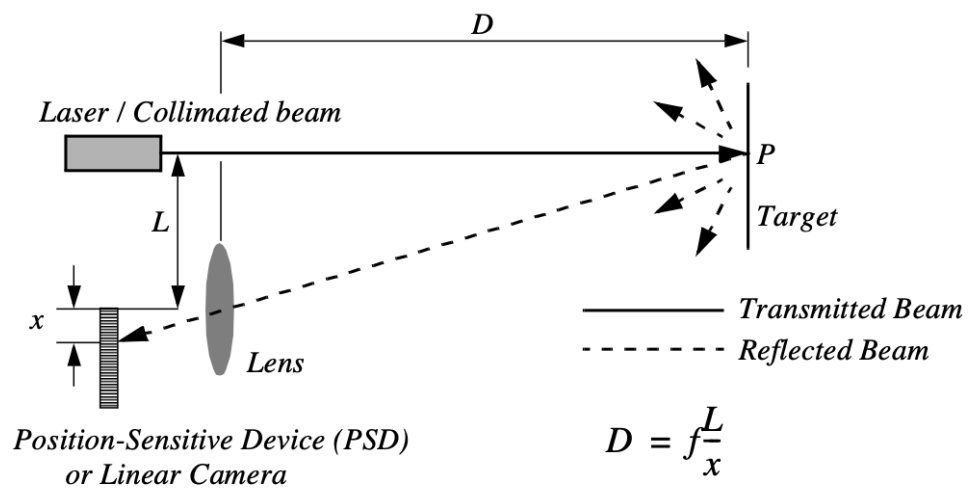


Figure 1.10: Principle of 1D laser triangulation.

beam is transmitted toward the target. The reflected light is collected by a lens and projected onto a position sensitive device<sup>12</sup> or linear camera. Given the geometry of **Fig. 1.10** the distance  $D$  is given by:

$$D = f \frac{L}{x}$$

The distance is proportional to  $\frac{1}{x}$ , therefore the sensor resolution is best for close objects and becomes poor at a distance. Sensors based on this principle are used in range sensing up to one or two m, but also in high precision industrial measurements with resolutions far below one  $\mu\text{m}$ . Optical triangulation devices can provide relatively high accuracy with very good resolution for close objects. However, the operating range of such a device is normally fairly limited by geometry. For example, an off-the-shelf optical triangulation sensor can operate over a distance range of between 8 cm and 80 cm. It is inexpensive compared to ultrasonic and laser rangefinder sensors.

Although more limited in range than sonar, the optical triangulation sensor has high bandwidth and does not suffer from cross-sensitivities that are more common in the sound domain.



<sup>12</sup>A position sensitive device and/or position sensitive detector is an optical position sensor which can measure a position of a light spot in one or two-dimensions on a sensor surface.

## Structured Light (2D Sensor)

If one replaced the linear camera or Position Sensing Device (PSD) of an optical triangulation sensor with a two-dimensional receiver such as a CCD or CMOS camera, then one can recover distance to a large set of points instead of to only one point. The emitter must project a known pattern, or structured light, onto the environment. Many systems exist which either project light textures (fig. 4.15b) or emit collimated light by means of a rotating mirror. Yet another popular alternative is to project a laser stripe (fig. 4.15a) by turning a laser beam into a plane using a prism. Regardless of how it is created, the projected light has a known structure, and therefore the image taken by the CCD or CMOS receiver can be filtered to identify the pattern's reflection.

The problem of recovering depth here far simpler than the problem of passive image analysis.

In passive image analysis, as we discuss later, existing features in the environment must be used to perform correlation, while the present method projects a **known pattern upon the environment** and thereby avoids the standard correlation problem altogether. Furthermore, the structured light sensor is an active device; so, it will continue to work in dark environments as well as environments in which the objects are **featureless<sup>13</sup>**. In contrast, stereo vision would fail in such texture-free circumstances. Figure 4.15c shows a one-dimensional active triangulation geometry. We can examine the trade-off in the design of triangulation systems by examining the geometry in figure 4.15c. The measured values in the system are  $\alpha$  and  $u$ , the distance of the illuminated point from the origin in the imaging sensor.<sup>14</sup> From figure 4.15c, simple geometry shows that:

$$x = \frac{bu}{f \cot \alpha - u} \quad \text{and} \quad z = \frac{bf}{f \cot \alpha - u}.$$

where  $f$  is the distance of the lens to the imaging plane. In the limit, the ratio of image resolution to range resolution is defined as the triangulation gain  $G_p$  and from equation 4.12 is given by:

$$\frac{\partial u}{\partial z} = G_p = \frac{bf}{z^2}$$

This shows that the ranging accuracy, for a given image resolution, is proportional to source/detector separation  $b$  and focal length  $f$ , and decreases with the square of the range  $z$ . In a scanning ranging system, there is an additional effect on the ranging accuracy, caused by the measurement of the projection angle  $\alpha$ . From equation 4.12 we see that:

$$\frac{\partial \alpha}{\partial z} = G_{ff} = \frac{b \sin \alpha^2}{z^2}$$

We can summarize the effects of the parameters on the sensor accuracy as follows:

**Baseline Length (b)** the smaller  $b$  is the more compact the sensor can be. The larger  $b$  is the better the range resolution will be. Note also that although these sensors do not suffer from

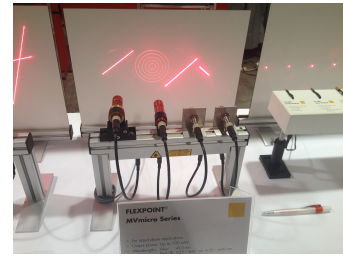


**Figure 1.11:** Structured light sources on display at the 2014 Machine Vision Show in Boston [5].

<sup>13</sup>e.g., uniformly coloured and possess no visible edge.

<sup>14</sup>the imaging sensor here can be a camera or an array of photo diodes of a position sensitive device (e.g. a 2D PSD

the correspondence problem, the disparity problem still occurs. As the baseline length  $b$  is increased, one introduces the chance that, for close objects, the illuminated point(s) may not be in the receiver's field of view.

**Detector length and focal length  $f$**  A larger detector length can provide either a larger field of view or an improved range resolution or partial benefits for both. Increasing the detector length however means a larger sensor head and worse electrical characteristics (increase in random error and reduction of bandwidth). Also, a short focal length gives a large field of view at the expense of accuracy and vice versa.

At one time, laser stripe-based structured light sensors were common on several mobile robot bases as an inexpensive alternative to laser rangefinding devices. However, with the increasing quality of laser rangefinding sensors in the 1990's the structured light system has become relegated largely to vision research rather than applied mobile robotics.

### 1.2.2 Motion and Speed Sensors

Some sensors directly measure the relative motion between the robot and its environment. Since such motion sensors detect **relative motion**, so long as an object is moving relative to the robot's reference frame, it will be detected and its speed can be estimated. There are a number of sensors that inherently measure some aspect of motion or change.



<sup>15</sup>An example of a pyroelectric sensor.

For example, a pyroelectric<sup>15</sup> sensor detects change in heat.

When someone walks across the sensor's field of view, his motion triggers a change in heat in the sensor's reference frame. In the next subsection, we describe an important type of motion detector based on the Doppler effect. These sensors represent a well-known technology with decades of general applications behind them.

For fast-moving AMRs such as autonomous highway vehicles and unmanned flying vehicles, Doppler-based motion detectors are the obstacle detection sensor of choice.

### Doppler Effect

Anyone who has noticed the change in siren pitch when an ambulance approaches and then passes by is familiar with the Doppler effect.<sup>16</sup>

A transmitter emits an electromagnetic or sound wave with a frequency  $f_t$ . It is either received by a receiver (fig. 4.16a) or reflected from an object (fig. 4.16b). The measured frequency  $f_r$  at the receiver is a function of the relative speed  $v$  between transmitter and receiver according to

$$f_r = f_t \frac{1}{1 + \frac{v}{c}}$$

<sup>16</sup>For anyone who needs a bit more information, it is the change in the frequency of a wave in relation to an observer who is moving relative to the source of the wave. The Doppler effect is named after the physicist Christian Doppler, who described the phenomenon in 1842. A common example of Doppler shift is the change of pitch heard when a vehicle sounding a horn approaches and recedes from an observer. Compared to the emitted frequency, the received frequency is higher during the approach, identical at the instant of passing by, and lower during the

if the transmitter is moving and

$$f_r = f_t \left( 1 + \frac{v}{c} \right)$$

if the receiver is moving. In the case of a reflected wave (fig. 4.16b) there is a factor of two introduced, since any change  $x$  in relative separation affects the round-trip path length by  $2x$ . Furthermore, in such situations it is generally more convenient to consider the change in frequency  $f$ , known as the Doppler shift, as opposed to the Doppler frequency notation above.

if the receiver is moving. In the case of a reflected wave (fig. 4.16b) there is a factor of two introduced, since any change  $x$  in relative separation affects the round-trip path length by  $2x$ . Furthermore, in such situations it is generally more convenient to consider the change in frequency  $f$ , known as the Doppler shift, as opposed to the Doppler frequency notation above.

$$\Delta f = f_t - f_r = \frac{2f_t v \cos \theta}{c} \quad \text{and} \quad v = \frac{\Delta f c}{2f_t \cos \theta}$$

where:  $f = f_t - f_r$  (4.17)  $v = \frac{\Delta f c}{2f_t \cos \theta}$  (4.18)  $\theta$  = relative angle between direction of motion and beam axis  $c$  = speed of sound or light  $f$  = Doppler frequency shift  $\Delta f$  = change in frequency  $v$  = velocity  $t$  = time. The Doppler effect applies to sound and electromagnetic waves. It has a wide spectrum of applications: Soundwaves: e.g. industrial process control, security, fishfinding, measurement of ground speed. Electromagnetic waves: e.g. vibration measurement, radar systems, object tracking. A current application area is both autonomous and manned highway vehicles. Both micro-wave and laser radar systems have been designed for this environment. Both systems have equivalent range, but laser can suffer when visual signals are deteriorated by environmental conditions such as rain, fog, etc. Commercial microwave radar systems are already available for installation on highway trucks. These systems are called VORAD (vehicle on-board radar) and have a total range of approximately 150m. With an accuracy of approximately 97%, these systems report range rate from 0 to 160 km/hr with a resolution of 1 km/hr. The beam is approximately 4° wide and 5° in elevation. One of the key limitations of radar technology is its bandwidth. Existing systems can provide information on multiple targets at approximately 2 Hz.

## 1.3 Vision Based Sensors

Vision is our most powerful sense. It provides us with an enormous amount of information about the environment and enables rich, intelligent interaction in dynamic environments. It is therefore not at all surprising that a great deal of effort has been devoted to providing machines with sensors which can at least try to mimic the capabilities of the human vision system.

The first step in this process is the creation of sensing devices that capture the same raw information which is the light the human vision system uses. The main topics which will be described are the two (2) current technologies for creating vision sensors:

1. CCD,
2. CMOS.

Of course, these sensors have specific limitations in performance compared to the human eye, and it is important to understand these limitations. Later sections describe vision-based sensors which are commercially available, similar to the sensors discussed previously, along with their disadvantages and most popular applications.

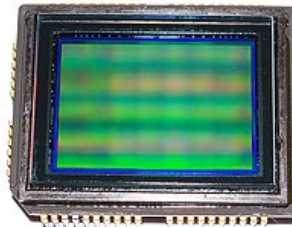


**Figure 1.12:** Sony ICX493AQ 10.14-megapixel APS-C (23.4 × 15.6 mm) CCD from digital camera Sony DSLR-A200 or DSLR-A300, sensor side [6].

### CCD and CMOS Sensors

When it comes to the marketplace, CCD is the most popular fundamental ingredient for robotic vision systems.<sup>17</sup> The CCD chip, which you can see in **Fig. 1.12** is an array of light-sensitive picture elements, or pixels, usually with between 20 000 and 2 million pixels total.

Each pixel can be thought of as a **light-sensitive, discharging capacitor** that is 5 to 25  $\mu\text{m}$  in size. First, the capacitors of all pixels are fully charged, then the integration period begins. As photons of light strike each pixel, the electrons are liberated, which are captured by electric fields and retained at the pixel. Over time, each pixel accumulates a varying level of charge based on the total number of photons that have struck it. After the integration period is complete, the relative charges of all pixels need to be **frozen and read**.

In a CCD, the reading process is performed at one corner of the CCD chip.<sup>18</sup> The bottom row of pixel charges are transported to this corner and read, then the rows above shift down and the process repeats. This means that each charge **must be transported across the chip**, and it is critical the value be preserved.

This requires specialised control circuitry and custom fabrication techniques to ensure the stability of transported charges.

The photo-diodes used in CCD chips<sup>19</sup> are **NOT** equally sensitive to all frequencies of light. They are sensitive to light between 400 nm and 1000 nm wavelength.<sup>20</sup>

<sup>19</sup>This also includes CMOS as well.

<sup>20</sup>This number range is usually given for easier numbers as both CCD and CMOS have sensitivity values at approximately 350 - 1050 nm.

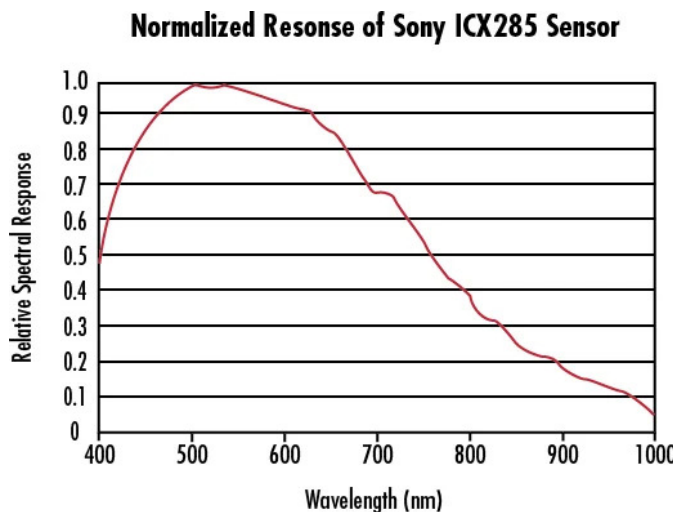


Figure 1.13: Normalized Spectral Response of a Typical Monochrome CCD.

It is important to remember that photodiodes are **less sensitive to the ultraviolet** part of the spectrum and are overly **sensitive to the infrared** portion (e.g. heat) which you can see in Fig. 1.13. You can see that the basic light-measuring process is colourless.<sup>21</sup>

There are two (2) common approaches for creating color images. If the pixels on the CCD chip are grouped into 2-by-2 sets of four (4), then red, green and blue dyes can be applied to a colour filter so each individual pixel receives only light of just one color.

<sup>21</sup>It is just measuring the total number of photons that strike each pixel in the integration period regardless whether the light hitting it is blue, red or green.

Normally, two (2) pixels measure green while one pixel each measures red and blue light intensity. Of course, this 1-chip color CCD has a geometric resolution disadvantage.

The number of pixels in the system has been effectively cut by a factor of 4, and therefore the image resolution output by the CCD camera will be sacrificed.

The 3-chip color camera avoids these problems by splitting the incoming light into three (3) complete<sup>22</sup> copies. Three separate CCD chips receive the light, with one red, green or blue filter over each entire chip. Thus, in parallel, each chip measures light intensity for just one color, and the camera must combine the CCD chips' outputs to create a joint color image.

<sup>22</sup>Albeit, with lower resolution.

Resolution is preserved in this solution, although the 3-chip color cameras are, as one would expect, significantly more expensive and therefore more rarely used in mobile robotics.

Both 3-chip and single chip color CCD cameras suffer from the fact that photo-diodes are much more sensitive to the near-infrared end of the spectrum. This means that the overall system detects blue light much more poorly than red and green. To compensate, the gain must be increased on the blue channel, and this introduces greater absolute noise on blue<sup>23</sup> than on red and green. It is not uncommon to assume at least 1 - 2 bits of additional noise on the blue channel.

<sup>23</sup>This is generally defined as the amplifier noise.

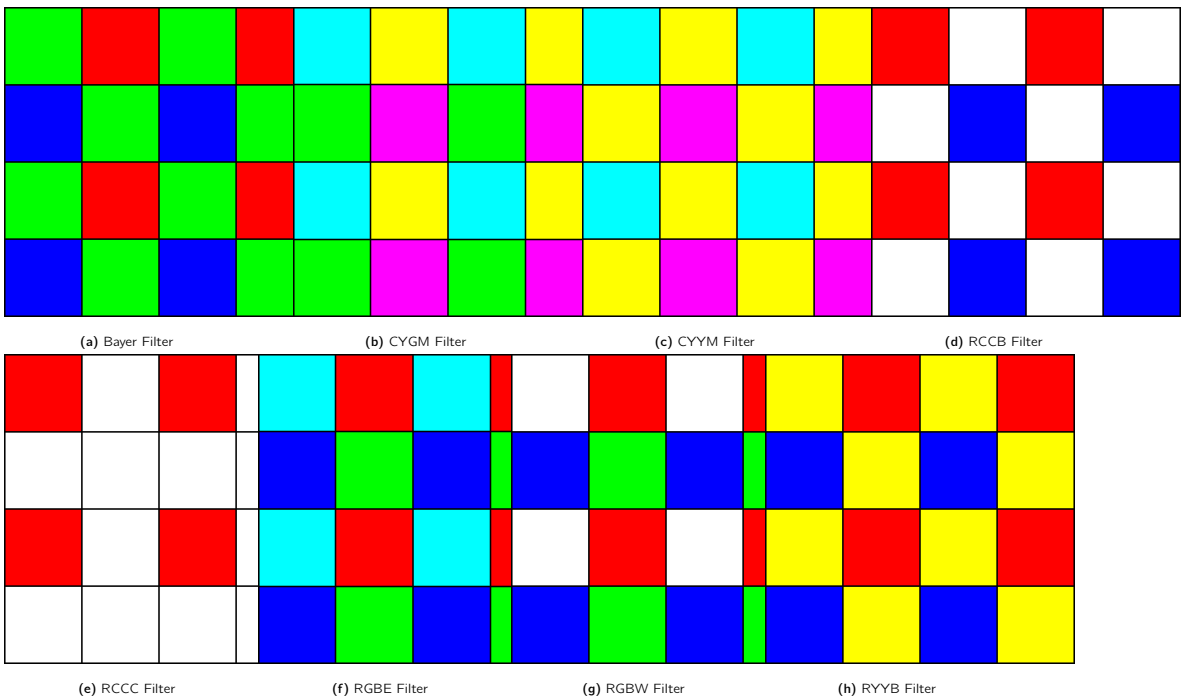


Figure 1.14: Types of colour filter used in commercial and industrial applications

The CCD camera has several camera parameters that affect its behavior. In some cameras, these parameter values are fixed. In others, the values are constantly changing based on built-in feedback loops. In higher-end cameras, the user can modify the values of these parameters via software embedded into the device.

<sup>24</sup>It's the speed at which the shutter of the camera closes. A fast shutter speed creates a shorter exposure - the amount of light the camera takes in - and a slow shutter speed gives a longer exposure.

The iris position and shutter speed<sup>24</sup> regulate the amount of light being measured by the camera. The iris is simply a mechanical aperture that constricts incoming light, just as in standard 35mm cameras. Shutter speed regulates the integration period of the chip. In higher-end cameras, the effective shutter speed can be as brief at 1/30,000s and as long as 2s. Camera gain controls the overall amplification of the analog signal, prior to A/D conversion. However, it is very important to understand that, even though the image may appear brighter after setting high gain, the shutter speed and iris may not have changed at all. Thus gain merely amplifies the signal, and amplifies along with the signal all of the associated noise and error. Although useful in applications where imaging is done for human consumption (e.g. photography, television), gain is of little value to a mobile roboticist.

In colour cameras, an additional control exists for white balance. Depending on the source of illumination in a scene<sup>25</sup> the relative measurements of red, green and blue light which combine to define pure white light will change dramatically which can be seen in **Fig. 1.15** which can also be adjusted with algorithms [8]. The human eyes compensate for all such effects in ways that are not fully understood, however, the camera can demonstrate glaring inconsistencies in which the same table looks blue in one image, taken during the night, and yellow in another image, taken during the day. White balance controls enable the user to change the relative gain for red, green and blue in order to maintain more consistent color definitions in varying contexts.

<sup>25</sup>For example this could be fluorescent lamps, incandescent lamps, sunlight, underwater filtered light, etc.

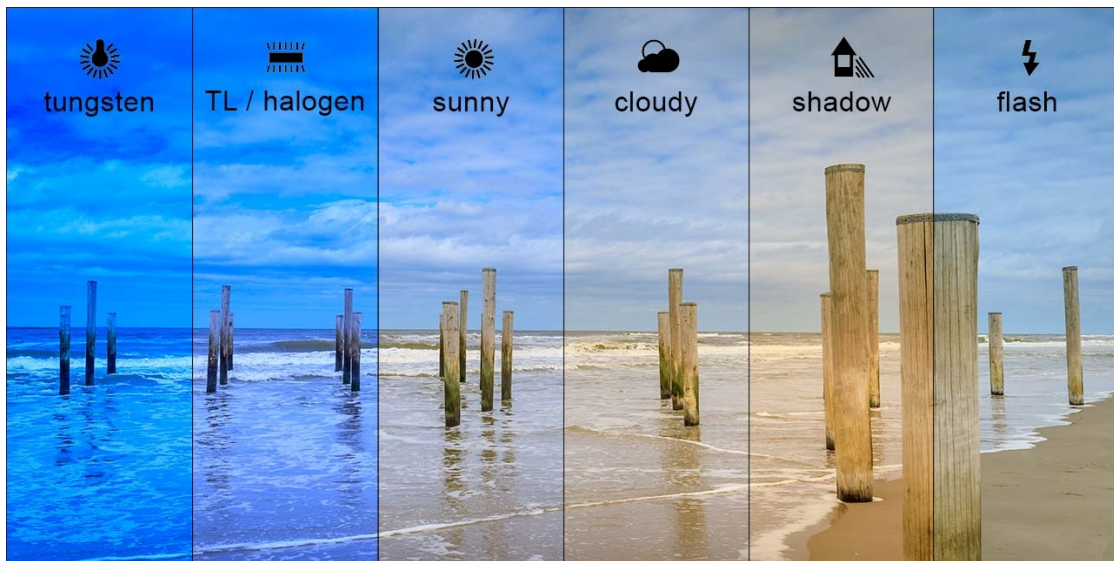


Figure 1.15: Example of white balance. Here the same scene is emulated to be shot under different light conditions [9].

The key disadvantages of CCD cameras are primarily in the areas of inconstancy and **dynamic range**.

### Dynamic Range

Dynamic range in photography describes the ratio between the maximum and minimum measurable light intensities (white and black, respectively). In the real world, one never encounters true white or black - only varying degrees of light source intensity and subject reflectivity. Therefore the concept of dynamic range becomes more complicated, and depends on whether you are describing a capture device (such as a camera or scanner), a display device (such as a print or computer display), or the subject itself.

As mentioned above, a number of parameters can change the brightness and colours with which a camera creates its image.

Manipulating these parameters in a way to provide consistency over time and over environments, for example ensuring a green shirt always looks green, and something dark grey is always dark grey, remains an open problem [10].

The second type of disadvantages relates to the behavior of a CCD chip in environments with **extreme illumination**. In cases of very low illumination, each pixel will receive only a small number of photons. The longest possible shutter speed and camera optics (i.e. pixel size, chip size, lens focal length and diameter) will determine the minimum level of light for which the signal is stronger than random error noise. In cases of very high illumination, a pixel fills its well with free electrons and, as the well reaches its limit, the probability of trapping additional electrons falls and therefore the linearity between incoming light and electrons in the well degrades. This is termed **saturation**<sup>26</sup> and can indicate the existence of a further problem related to cross-sensitivity [12]. When a well has reached its limit, then additional light within the remainder of the integration period may cause



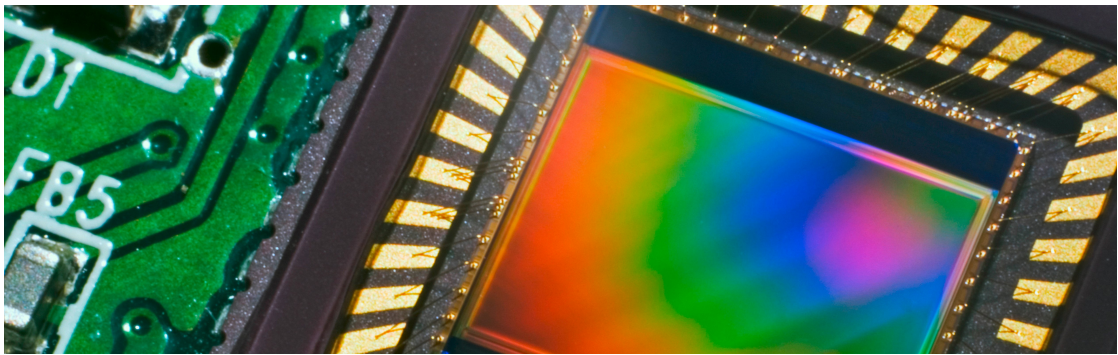


Figure 1.16: A close-up view of a CMOS sensor and its circuitry [13].

further charge to leak into neighbouring pixels, causing them to report incorrect values or even reach secondary saturation. This effect, called blooming, means that individual pixel values are **NOT** truly **independent**. The camera parameters may be adjusted for an environment with a particular light level, but the problem remains that the dynamic range of a camera is limited by the well capacity of the individual pixels.

For example, a high quality CCD may have pixels that can hold 40 000 electrons. The noise level for reading the well may be 11 electrons, and therefore the dynamic range will be 40,000:11, or 3,600:1, which is 35 dB.

### 1.3.1 CMOS Technology

The Complementary Metal Oxide Semiconductor (CMOS) chip is a significant departure from the CCD. Similar to CCD, it too has an array of pixels, but located alongside each pixel are **several transistors specific to that pixel**. Just as in CCD chips, all of the pixels accumulate charge during the integration period. During the data collection step, the CMOS takes a new approach:

The pixel-specific circuitry next to every pixel measures and amplifies the pixel's signal, all in parallel for every pixel in the array.

Using more traditional traces from general semiconductor chips, the resulting pixel values are all carried to their destinations. CMOS has a number of advantages over CCD technologies. First and foremost, there is no need for the specialized clock drivers and circuitry required in the CCD to transfer each pixel's clock down all of the array columns and across all of its rows.<sup>27</sup>

This also means that specialized semiconductor manufacturing processes are not required to create CMOS chips.



<sup>27</sup>-CAM80CUNX is an 8MP Ultra-lowlight MIPI CSI-2 camera capable of streaming 4K @ 44 fps.

This 8MP camera is based on SONY STARVIS IMX415 CMOS image sensor [14]

Therefore, the same production lines that create microchips can create inexpensive CMOS chips as well. The CMOS chip is so much simpler that it consumes significantly less power, it operates with a power consumption a tenth the power consumption of a CCD chip [15].

In a AMR, power is a scarce resource and therefore this is an important advantage.

On the other hand, the CMOS chip also faces several disadvantages.

- Most importantly, the circuitry next to each pixel consumes valuable real estate on the face of the light-detecting array. Many photons hit the transistors rather than the photodiode, making the CMOS chip significantly less sensitive than an equivalent CCD chip.
- CMOS, compared to CCD is still finding ground in the marketplace, and as a result, the best resolution that one can purchase in CMOS format continues to be far inferior to the best CCD chips available.
- CMOS sensors have a lower dynamic range,
- CMOS sensors have higher levels of noise.

1

2

Compared to the human eye, these chips all have worse performance, cross-sensitivity and a limited dynamic range. As a result, vision sensors today continue to be fragile. Only over time, as the underlying performance of imaging chips improves, will significantly more robust vision-based sensors for AMRs be available.

### Shot Noise

Shot noise or Poisson noise is a type of noise which can be modeled by a Poisson process. In electronics shot noise originates from the discrete nature of electric charge. Shot noise also occurs in photon counting in optical devices, where shot noise is associated with the particle nature of light.



**Figure 1.17:** Photon noise simulation. Number of photons per pixel increases from left to right and from upper row to bottom row [16].

### 1.3.2 Visual Ranging Sensors

Range sensing is extremely important in AMR as it is a basic input for successful obstacle avoidance. As we have seen earlier, a number of sensors are popular in robotics specifically for their ability to recover depth estimates:

ultrasonic, laser rangefinder, optical rangefinder, etc.

It is natural to attempt to implement ranging functionality using vision chips as well. However, a fundamental problem with visual images makes rangefinding relatively difficult.

Any vision chip collapses the three-dimensional world into a two-dimensional image plane, thereby losing depth information. If one can make strong assumptions regarding the size of objects in the world, or their particular colour and reflectance, then one can directly interpret the appearance of the two-dimensional image to recover depth. But such assumptions are rarely possible in real-world AMR applications.

Without such assumptions, a single picture does not provide enough information to recover spatial information.

The general solution is to recover depth by looking at several images of the scene to gain more information, which will be hopefully enough to at least partially recover depth. The images used **must be different**, so that taken together they provide additional information. They could differ in viewpoint, which would allow the use of stereo or motion algorithms.

An alternative is to create different images, not by changing the viewpoint, but by changing the camera geometry, such as the focus position or lens iris. This is the fundamental idea behind depth from focus and depth from defocus techniques. We will now look into the general approach to the depth from focus techniques as it presents a straightforward and efficient way to create a vision-based range sensor.

### 1.3.3 Depth from Focus

The depth from focus class of techniques relies on the fact that image properties not only change as a function of the **scene**, but also as a function of the **camera parameters**. The relationship between camera parameters and image properties is depicted in **Fig. 1.18**. The fundamental formula governing image formation relates the distance of the object from the lens,  $d$  in **Fig. 1.18**, to the distance  $e$  from the lens to the focal point, based on the focal length  $f$  of the lens:

$$\frac{1}{f} = \frac{1}{d} + \frac{1}{e}$$

<sup>28</sup>A three-dimensional counterpart to a pixel. If the image plane is located at distance  $e$  from the lens, then for the specific object voxel<sup>28</sup> depicted, all light will be focused at a single point on the image plane and the object voxel will be focused. However, when the image plane is **NOT** at  $e$ , as is seen in **Fig. 1.18**, then the light

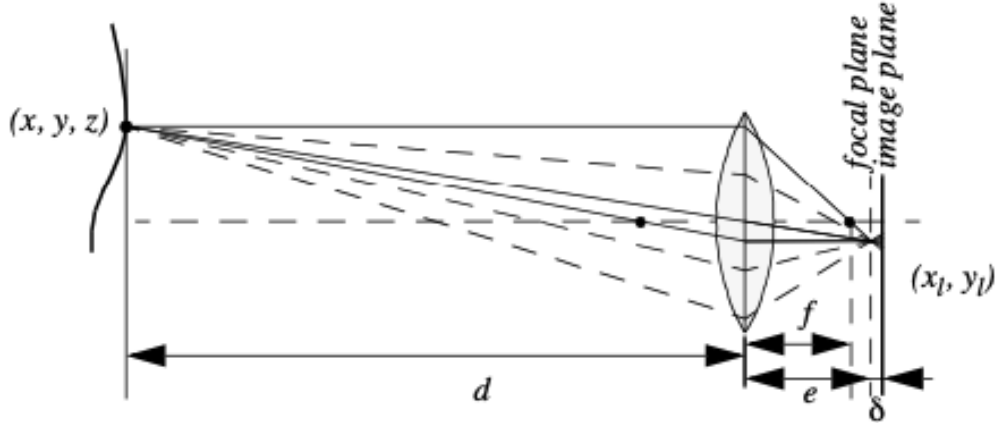


**Figure 1.18:** Depiction of the camera optics and its impact on the image. To get a sharp image, the image plane must coincide with the focal plane. Otherwise the image of the point  $(x, y, z)$  will be blurred in the image as can be seen in the drawing above.

from the object voxel will be cast on the image plane as a **blur circle**. To a first approximation, the light is homogeneously distributed throughout this blur circle, and the radius  $R$  of the circle can be characterized according to the equation:

$$R = \frac{L\delta}{2e}$$

where  $L$  is the diameter of the lens or aperture and  $\delta$  is the displacement of the image plan from the focal point.

Given these formulae, several basic optical effects are clear.

For example, if the aperture<sup>29</sup> or lens is reduced to a point, as in a pin-hole camera, then the radius of the blur circle approaches zero.

This is consistent with the fact that decreasing the iris aperture opening causes the depth of field to increase until all objects are in focus. Of course, the disadvantage of doing so is that we are allowing less light to form the image on the image plane and so this is practical only in bright circumstances. The second property to be deduced from these optics equations relates to the sensitivity of blurring as a function of the distance from the lens to the object.

<sup>29</sup>The aperture is the opening in the lens that allows light to enter the camera and onto the sensor or film.



**Figure 1.19:** Three images of the same scene taken with a camera at three different focusing positions. Note the significant change in texture sharpness between the near surface and far surface [17].

Suppose the image plane is at a fixed distance  $L = 1.2$  from a lens with diameter  $L = 0.2$  and focal length  $f = 0.5$ . We can see from Equation (4.20) that the size of the blur circle  $R$  changes proportionally with the image plane displacement. If the object is at distance  $d = 1$ , then from Equation (4.19) we can compute  $e=1$  and therefore  $R = 0.2$ . Increase the object distance to  $d = 2$  and as a result  $R = 0.533$ . Using Equation (4.20) in each case we can compute  $R = 0.02$   $R = 0.08$  respectively. This demonstrates high sensitivity for defocusing when the object is close to the lens. In contrast suppose the object is at  $d = 10$ . In this case we compute  $e = 0.526$ . But if the object is again moved one unit, to  $d = 11$ , then we compute  $e = 0.524$ . Then resulting blur circles are  $R = 0.117$  and  $R = 0.129$ , far less than the quadrupling in  $R$  when the obstacle is  $1/10$  the distance from the lens. This analysis demonstrates the fundamental limitation of depth from focus techniques: they lose sensitivity as objects move further away (given a fixed focal length). Interestingly, this limitation will turn out to apply to virtually all visual ranging techniques, including depth from stereo and depth from motion. Nevertheless, camera optics can be customized for the depth range of the intended application. For example, a "zoom" lens with a very large focal length  $f$  will enable range resolution at significant distances, of course at the expense of field of view. Similarly, a large lens diameter, coupled with a very fast shutter speed, will lead to larger, more detectable blur circles. Given the physical effects summarized by the above equations, one can imagine a visual ranging sensor that makes use of multiple images in which camera optics are varied (e.g. image plane displacement) and the same scene is captured (see Fig. 4.20). In fact this approach is not a new invention. The human visual system uses an abundance of cues and techniques, and one system demonstrated in humans is depth from focus. Humans vary the focal length of their lens continuously at a rate of about 2 Hz. Such approaches, in which the lens optics are actively searched in order to maximize focus, are technically called depth from focus. In contrast, depth from defocus means that depth is recovered using a series of images that have been taken with different camera geometries. Depth from focus methods are one of the simplest visual ranging techniques. To determine the range to an object, the sensor simply moves the image plane (via focusing) until maximizing the sharpness of the object. When the sharpness is maximized, the corresponding position of the image plane directly reports range. Some autofocus cameras and virtually all autofocus video cameras use this technique. Of course, a method is required for measuring the sharpness of an image or an object within the image. The most common techniques are approximate measurements of the sub-image gradient:

$$\text{sharpness}_1 = \sum_{x,y} |I(x, y) - I(x-1, y)| \quad (1.3)$$

$$\text{sharpness}_2 = \sum_{x,y} (I(x, y) - I(x-2, y-2))^2 \quad (1.4)$$

A significant advantage of the horizontal sum of differences technique (Equation (4.21)) is that the calculation can be implemented in analog circuitry using just a rectifier, a low-pass filter and a high-pass filter. This is a common approach in commercial cameras and video recorders. Such systems will be sensitive to contrast along one particular axis, although in practical terms this is rarely an issue. However depth from focus is an active search method and will be slow because it takes time to change the focusing parameters of the camera, using for example a servo-controlled focusing ring. For this reason this method has not been applied to AMRs. A variation of the depth from focus technique has been applied to a AMR, demonstrating obstacle avoidance in a variety of environments as well as avoidance of concave obstacles such as steps and ledges [95]. This robot

uses three monochrome cameras placed as close together as possible with different, fixed lens focus positions (Fig. 4.21).

Several times each second, all three frame-synchronized cameras simultaneously capture three images of the same scene. The images are each divided into five columns and three rows, or 15 subregions. The approximate sharpness of each region is computed using a variation of Equation (4.22), leading to a total of 45 sharpness values. Note that Equation 22 calculates sharpness along diagonals but skips one row. This is due to a subtle but important issue. Many cameras produce images in interlaced mode. This means that the odd rows are captured first, then afterwards the even rows are captured. When such a camera is used in dynamic environments, for example on a moving robot, then adjacent rows show the dynamic scene at two different time points, differing by up to 1/30 seconds. The result is an artificial blurring due to motion and not optical defocus. By comparing only even-number rows we avoid this interlacing side effect.

Recall that the three images are each taken with a camera using a different focus position. Based on the focusing position, we call each image close, medium or far. A  $5 \times 3$  coarse depth map of the scene is constructed quickly by simply comparing the sharpness values of each three corresponding regions. Thus, the depth map assigns only two bits of depth information to each region using the values close, medium and far. The critical step is to adjust the focus positions of all three cameras so that flat ground in front of the obstacle results in medium readings in one row of the depth map. Then, unexpected readings of either close or far will indicate convex and concave obstacles respectively, enabling basic obstacle avoidance in the vicinity of objects on the ground as well as drop-offs into the ground. Although sufficient for obstacle avoidance, the above depth from focus algorithm presents unsatisfyingly coarse range information. The alternative is depth from defocus, the most desirable of the focus-based vision techniques. Depth from defocus methods take as input two or more images of the same scene, taken with different, known camera geometry. Given the images and the camera geometry settings, the goal is to recover the depth information of the three-dimensional scene represented by the images. We begin by deriving the relationship between the actual scene properties (irradiance and depth), camera geometry settings and the image  $g$  that is formed at the image plane. The focused image  $f(x,y)$  of a scene is defined as follows. Consider a pinhole aperture ( $L=0$ ) in lieu of the lens. For every point  $p$  at position  $(x,y)$  on the image plane, draw a line through the pinhole aperture to the corresponding, visible point  $P$  in the actual scene. We define  $f(x,y)$  as the irradiance (or light intensity) at  $p$  due to the light from  $P$ . Intuitively,  $f(x,y)$  represents the intensity image of the scene perfectly in focus



# Glossary

**AMR** Autonomous Mobile Robotics. i, 5–13, 15–21, 23, 26, 33, 34, 36

**CCD** Charge Coupled Device. i, v, 6, 10, 25, 28–33

**CMOS** Complimentary MOS. i, v, 25, 28, 29, 32, 33

**DoF** Degrees of Freedom. i

**GPS** Global Positioning System. i, 16

**LED** Light-Emitting Diode. i, 22

**LIDAR** Light Detection and Ranging. i, 21

**PSD** Position Sensing Device. i, 25

**ToF** Time-of-Flight. i, 18, 19, 21



# Glossary

**AMR** Autonomous Mobile Robotics. i, 5–13, 15–21, 23, 26, 33, 34, 36

**CCD** Charge Coupled Device. i, v, 6, 10, 25, 28–33

**CMOS** Complimentary MOS. i, v, 25, 28, 29, 32, 33

**DoF** Degrees of Freedom. i

**GPS** Global Positioning System. i, 16

**LED** Light-Emitting Diode. i, 22

**LIDAR** Light Detection and Ranging. i, 21

**PSD** Position Sensing Device. i, 25

**ToF** Time-of-Flight. i, 18, 19, 21



# Bibliography

- [1] Farnell. *Rotary Encoder, Module, Optical, Incremental, 500 PPR, 0 Detents, Vertical, Without Push Switch*. 2025. URL: <https://at.farnell.com/en-AT/broadcom-limited/aedb-9140-a13/encoder-3channel-500cpr-8mm/dp/1161087>.
- [2] Flyrobo. *GY-26 Digital Electronic Compass Sensor Module*. 2025. URL: <https://www.flyrobo.in/gy-26-digital-electronic-compass-sensor-module>.
- [3] FindLight. *Optical Gyroscopes: Measuring Rotational Changes With Sagnac Effect*. 2025. URL: <https://www.findlight.net/blog/optical-gyroscopes-measuring-rotations/>.
- [4] PiHut. *HC-SR04 Ultrasonic Range Sensor on the Raspberry Pi*. 2025. URL: <https://thepihut.com/blogs/raspberry-pi-tutorials/hc-sr04-ultrasonic-range-sensor-on-the-raspberry-pi>.
- [5] Reinhold. *Structured light sources on display at the 2014 Machine Vision Show in Boston*. 2014. URL: [https://commons.wikimedia.org/wiki/File:Structured\\_light\\_sources.agr.jpg](https://commons.wikimedia.org/wiki/File:Structured_light_sources.agr.jpg).
- [6] Andrzej. *CCD image sensor SONY ICX493AQA 10,14 (Gross 10,75) M pixels APS-C 1.8" 28.328mm (23.4 x 15.6 mm) from module IS-026 from digital camera SONY DSLR-A200 or DSLR-A300 sensor side*. 2014. URL: [https://commons.wikimedia.org/wiki/File:CCD\\_SONY\\_ICX493AQA\\_sensor\\_side.jpg](https://commons.wikimedia.org/wiki/File:CCD_SONY_ICX493AQA_sensor_side.jpg).
- [7] TeledyneCCD. *How a Charge Coupled Device (CCD) Image Sensor Works*. 2020. URL: [https://www.teledyneimaging.com/media/1300/2020-01-22\\_e2v\\_how-a-charge-coupled-device-works\\_web.pdf](https://www.teledyneimaging.com/media/1300/2020-01-22_e2v_how-a-charge-coupled-device-works_web.pdf).
- [8] K. Hirakawa and T.W. Parks. "Chromatic adaptation and white-balance problem". In: *IEEE International Conference on Image Processing 2005*. Vol. 3. 2005, pp. III–984. DOI: 10.1109/ICIP.2005.1530559.
- [9] Fstoppers. *Is There a Difference Between Color Temperature and White Balance?* 2022. URL: <https://fstoppers.com/natural-light/there-difference-between-color-temperature-and-white-balance-596031>.
- [10] Adrian Ilie and Greg Welch. "Ensuring color consistency across multiple cameras". In: *Tenth IEEE International Conference on Computer Vision (ICCV'05) Volume 1*. Vol. 2. IEEE. 2005, pp. 1268–1275.
- [11] Teledyne. *Saturation and Blooming*. 2025. URL: <https://www.photometrics.com/learn/imaging-topics/saturation-and-blooming>.

- [12] Zhen Zhang et al. "Analysis and simulation to excessive saturation effect of CCD". In: *2nd International Symposium on Laser Interaction with Matter (LIMIS 2012)*. Vol. 8796. SPIE. 2013, pp. 96–102.
- [13] Baumer. *Operating principle and features of CMOS sensors*. 2025. URL: <https://www.baumer.com/int/en/service-support/function-principle/operating-principle-and-features-of-cmos-sensors/a/EMVA1288>.
- [14] econ Systems. *CMOS camera module*. <https://www.directindustry.com/prod/e-con-systems/product-168594-2365044.html>. URL: <https://www.directindustry.com/prod/e-con-systems/product-168594-2365044.html>.
- [15] TS Holst and GC Lomheim. *CMOS/CCD Sensors*. JCD publishing, 2007.
- [16] Mdf. *A photon noise simulation*. 2010. URL: <https://commons.wikimedia.org/wiki/File:Photon-noise.jpg>.
- [17] Mark-j. *Open Camera Blog*. 2018. URL: <https://sourceforge.net/p/opencamera/blog/2018/09/focus-bracketing-with-open-camera/>.

